ACS APPLIED MATERIALS & INTERFACES

Research Article

www.acsami.org

High Capacitance, Photo-Patternable Ion Gel Gate Insulators Compatible with Vapor Deposition of Metal Gate Electrodes

Jae-Hong Choi,[†] Yuanyan Gu,[†] Kihyon Hong,[‡] Wei Xie,[‡] C. Daniel Frisbie,*[,‡] and Timothy P. Lodge*[,†,‡]

[†]Department of Chemistry, University of Minnesota, 207 Pleasant Street SE, Minneapolis, Minnesota 55455, United States

[‡]Department of Chemical Engineering and Materials Science, University of Minnesota, 421 Washington Avenue SE, Minneapolis, Minnesota 55455, United States

Supporting Information

ABSTRACT: A facile fabrication route to pattern high-capacitance electrolyte thin films in electrolyte-gated transistors (EGTs) was demonstrated using a photoinitiated cross-linkable ABA-triblock copolymer ion gel. The azide groups of poly(styrene-*r*-vinylbenzylazide) (PS-N_3) end-blocks can be chemically cross-linked via UV irradiation (λ = 254 nm) in the self-assembly of poly[(styrene-*r*-vinylbenzylazide)-*b*-ethylene oxide-*b*-(styrene-*r*-vinylbenzylazide)] (SOS-N_3) triblock copolymer in the ionic liquid 1-ethyl-3-methylimidazolium bis(trifluoromethylsulfonyl)imide ([EMI][TFSI]). Impedance spectroscopy and small-angle X-ray scattering revealed that ion transport and microstructure of the ion gel are not affected by UV cross-linking. Using a photoinduced cross-linking strategy, photopatterning of ion gels through a patterned mask was achieved. Employing a photopatterned ion gel as the high-capacitance gate insulator in thin film transistors (TFTs), arrays of TFTs exhibited uniform and high device performance. Specifically, both p-type (poly(3-hexylthiophene)) (P3HT) and n-type (ZnO) transistors displayed high carrier mobility (hole mobility of ~1.4 cm^2/ (V s) and electron mobility of ~0.7 cm^2/ (V s) and ON/OFF current ratio (~10^5) at supply voltages below 2 V. This study suggests that photopatterning is a promising candidate to conveniently incorporate high-capacitance ion gels into TFTs in the fabrication of printed electronics.

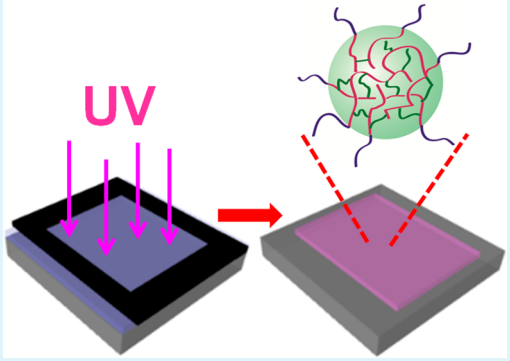

KEYWORDS: *photopatterning, chemical cross-linking, ion gel, thin-film transistor, metal gate electrode*

INTRODUCTION

The use of electrolytes as gate insulators in transistors has attracted much attention for printed electronics because it allows low voltage operation and offers flexibility, transparency, and low-cost processing.[1−15] Electrolytes serving as dielectrics in thin film transistors (TFTs) are ionically conducting but electronically insulating. They provide high capacitance by forming nanometer-thick electric double layers (EDLs) at the electrolyte/semiconductor and gate/electrolyte interfaces under applied gate voltages. Because the charge induced in the semiconductor channel is directly related to the specific capacitance of a gate dielectric, electrolyte gating with exceptionally large capacitance leads not only to a dramatic decrease in the operating voltage but also to an increase in the source−drain current.[16,17] Among various electrolyte dielectrics, ion gels comprising of a polymer network swollen with an ionic liquid have been successfully used to gate both organic[18−25] and inorganic[26−32] semiconductors by utilizing their exceptional properties including high ionic conductivity, wide electrochemical window, chemical and thermal stability, and ease of processing.

A physically cross-linked ion gel can be achieved through the assembly of ABA triblock copolymers with ionic liquid insoluble A end blocks and a soluble B middle block.[33] The structure and properties of ion gels can be controlled easily by tuning the polymer chemical structure, block length and architecture. Using such versatile physically cross-linked ion gels, our groups have recently developed several strategies for incorporating ion gels into TFTs, including aerosol jet printing,[4,19,30] lamination ("cut and stick" processing),[20] and transfer printing.[21] Although these methods have been successfully employed in high performance TFTs and have provided a wider variety of choices in ion gel processing, each method has both advantages and limitations. For example, the ion gel feature size and placement can be controlled easily by direct-write aerosol jet printing,[4,19,30] but so far aerosol jet printing is not a widely available technique for device fabrication. Likewise, thermo-reversible ion gels enable transfer printing of patterned ion gel layers using an elastomeric stamp, yet complex photolithographic processes are needed to make the patterned stamp.[21] Finally, mechanically free-standing ion gels can be cut by a razor blade and laminated conveniently on a semiconductor using tweezers, but precision control over feature size and placement is limited.[20]

Received: August 7, 2014
Accepted: October 6, 2014
Published: October 16, 2014

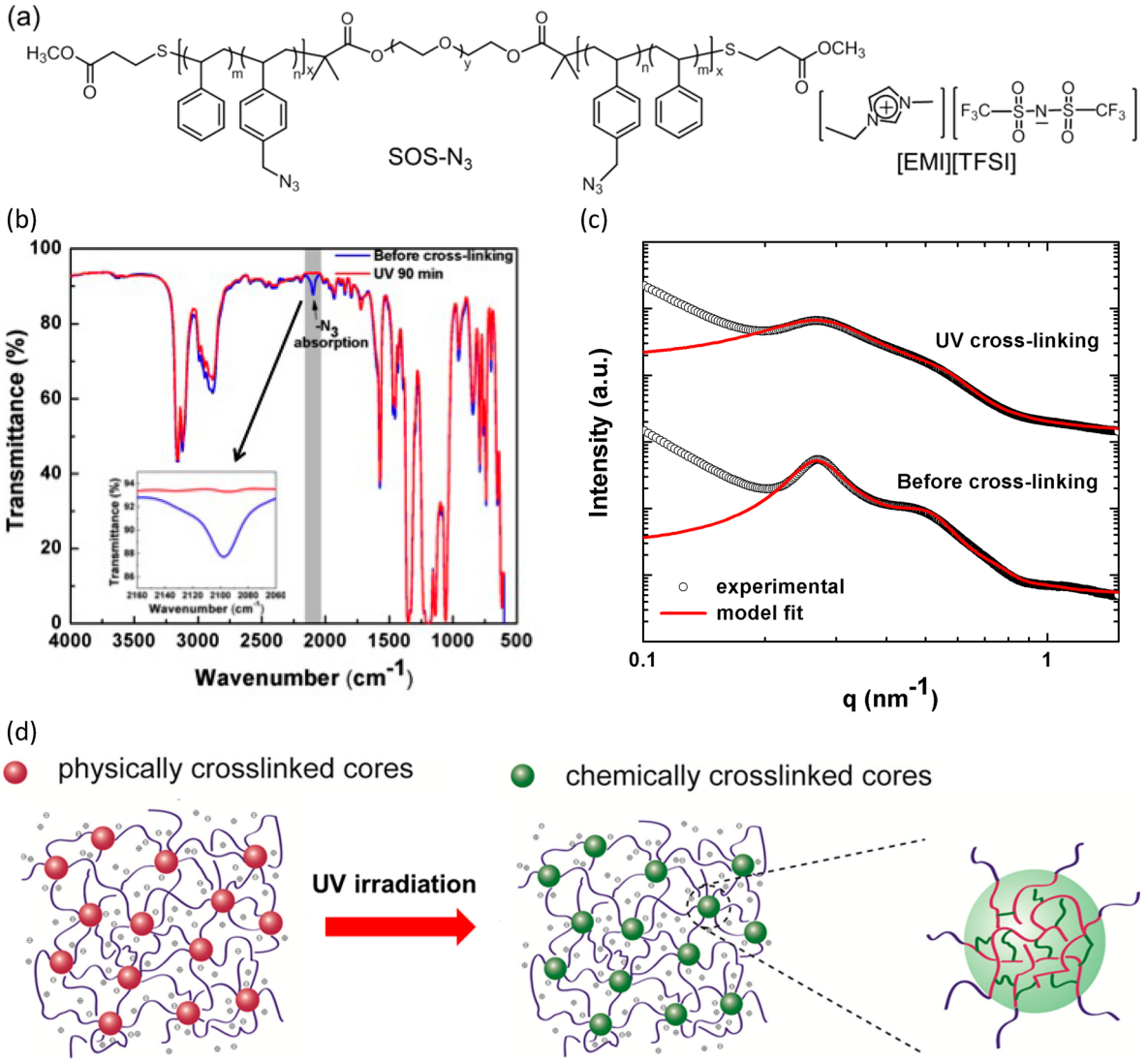

Figure 1. (a) Chemical structures of the chemically cross-linkable triblock copolymer, poly[(styrene-*r*-vinylbenzyl azide)-*b*-ethylene oxide-*b*-(styrene-*r*-vinylbenzyl azide)] (SOS-N_3) and ionic liquid, 1-ethyl-3-methylimidazolium bis(trifluoromethylsulfonyl)imide ([EMI][TFSI]). (b) FT-IR spectra of 10 wt % SOS-N_3 ion gel films before cross-linking and after UV irradiation for 90 min. The gray area indicates the absorption peak of azide groups. The inset shows the expanded IR spectra in the range of 2160−2060 cm^{-1}. (c) Small-angle X-ray scattering profiles as a function of scattering vector q for 10 wt % SOS-N_3 ion gels before cross-linking and after UV irradiation for 90 min. The experimental SAXS data (open circles) were fit to the Percus−Yevick hard sphere model (red solid line). (d) Schematic of chemical cross-linking of SOS-N_3 ion gels by UV irradiation.

In this paper, we demonstrate convenient photolithographic patterning of electrolyte thin films using a photoinitiated cross-linkable ABA-triblock copolymer ion gel. The ion gel comprises poly[(styrene-*r*-vinylbenzylazide)-*b*-ethylene oxide-*b*-(styrene-*r*-vinylbenzylazide)] (SOS-N_3) triblock copolymer in the ionic liquid, 1-ethyl-3-methylimidazolium bis-(trifluoromethylsulfonyl)imide ([EMI][TFSI]), and the azide groups of the poly(styrene-*r*-vinylbenzylazide) (PS-N_3) end-blocks can be chemically cross-linked via UV irradiation. Using this chemical cross-linking strategy, we demonstrate the ability to photopattern ion gels with a simple mask and we fabricate an array of TFTs with photopatterned ion gels as high-capacitance gate insulators. The TFTs exhibit excellent low voltage characteristics. The principal advantages of this novel material and patterning process are that (1) photopatterning is currently a more general and accessible approach in device fabrication than direct-write printing, (2) additional photolithographic steps with a photoresist are not required to make an ion gel pattern, (3) the photopatterned ion gel layers are amenable to subsequent materials deposition (even metal vapor deposition), and (4) the thickness of the gel can be tuned easily by varying the spin-coating conditions.

EXPERIMENTAL SECTION

Materials. Poly[(styrene-*r*-vinylbenzyl azide)-*b*-ethylene oxide-*b*-(styrene-*r*-vinylbenzyl azide)] (SOS-N_3(3.8−35−3.8)) was synthesized via reversible addition−fragmentation chain transfer (RAFT) polymerization and postpolymerization reaction. The detailed synthetic procedures have been described in a previous report.[34] Numbers in parentheses are the number-average molecular weights of each block in kg/mol. The ionic liquid 1-ethyl-3-methylimidazolium bis(trifluoromethylsulfonyl)imide [EMI][TFSI] was synthesized via an anion exchange reaction.[35] The ionic liquid was dried in a vacuum oven at 70 °C and stored in a glovebox or vacuum desiccator to minimize water contamination. The SOS-N_3 ion gel films were prepared using a solution-casting (spin-coating or drop-casting) technique from a solution prepared by codissolving SOS-N_3 polymer and [EMI][TFSI] in ethyl acetate at a 1:9:10 ratio(w/w/w). A ZnO

solution was prepared by dissolving zinc oxide powder (Sigma-Aldrich) in ammonium hydroxide (6 mg/mL), which was then stored in refrigerator for 1 day before using.[36] The thicknesses of ion gel and ZnO films were measured by a KLA-Tencor P-16 surface profiler.

Impedance Measurement and Fourier Transform Infrared (FTIR) Spectroscopy. Impedance properties of metal-ion gel-metal (MIM) capacitors were measured using electrochemical impedance spectroscopy (EIS; Solartron 1255B impedance analyzer, SI 1287 electrochemical interface, Zplot software). Measurements were conducted over a frequency range of $1-10^6$ Hz with an AC amplitude of 10 mV at room temperature. FT-IR measurements were performed on a Nicolet iS5 FT-IR spectrometer (Thermo Scientific) over a wavenumber range of 600–4000 cm^{-1} at room temperature. An ion gel film with a thickness of ca. 30 μm was prepared on a polished NaCl salt plate by drop casting for FT-IR analysis.

Device Fabrication. Source and drain electrodes (5.0 nm Cr/30.0 nm Au) were photolithographically patterned on SiO_2/Si substrates. The channel length and width were 10 and 1000 μm, respectively. The substrate was sequentially cleaned with acetone and isopropyl alcohol, and then dried with nitrogen gas. A ZnO precursor solution was spin-coated at a spin speed of 3000 rpm for 30 s on the Au electrodes, followed by annealing at 300 °C for 1 h under ambient conditions to generate ZnO. To generate hydroxyl groups on the ZnO surface, we treated the prepared ZnO films using a plasma cleaner (Harrick Plasma, PDC-32G). Then, UV-cross-linkable SOS-N_3 ion gel films were spin-coated onto the ZnO film at 1300 rpm for 45 s. Using a shadow mask, UV cross-linking of the ion gel on a selected area was conducted using a UVGL-55 hand-held UV lamp (UVP Inc., intensity =1.29 mW/cm^2 at 254 nm) for 40–60 min under an inert atmosphere, and then ion gel patterns were obtained by removing the unexposed part of ion gel (uncross-linked ion gel) with organic solvents (chloroform or ethyl acetate). Finally, a 100 nm thick Au gate electrode was deposited on patterned ion gels by thermal evaporation through a shadow mask. For devices fabricated partially by printing, all processes in device fabrication were the same as methods described above. Only regioregular poly(3-hexylthiophene) (P3HT) semiconducting films were deposited by aerosol-jet printing (Optomec, Inc.) following experimental procedures reported elsewhere.[19,30]

Electrical Measurement. Current–voltage ($I-V$) characteristics of transistors were collected using Keithley 236 and 6517 electrometers in combination with a Desert Cryogenics (Lakeshore, Inc.) vacuum probe station in a N_2-filled glovebox. All measurements were conducted in vacuum at a pressure of $<1 \times 10^{-6}$ Torr.

RESULTS AND DISCUSSION

Figure 1a shows the chemical structures of a SOS-N_3 triblock copolymer and EMI-TFSI ionic liquid. The azide functionality in the PS end-blocks can be chemically cross-linked via UV irradiation or annealing at elevated temperature.[37–39] The self-assembly of SOS-N_3 in EMI-TFSI forms a physically cross-linked ion gel where PS-N_3 cores act as cross-linking junctions interconnected by ionic liquid-soluble PEO chains. After annealing at 200 °C for 20 min, a chemically cross-linked ion gel can be attained from this physically cross-linked ion gel by thermal cross-linking of the azide groups in the cores.[34] To cross-link the ion gel only over selected areas and to process materials at lower temperature, an alternative cross-linking method is desired, which we achieve here via UV irradiation.

The cross-linking reaction of the azide groups in SOS-N_3 ion gels was examined using FT-IR. Solution cast ion gel samples on a polished NaCl salt plate were exposed to UV irradiation (intensity = 1.29 mW/cm^2 at 254 nm) for 90 min in a glovebox. The absorption peak for the azide group at ~2095 cm^{-1} disappeared after UV exposure, which indicates the azide groups in the end-blocks of the 10 wt % SOS-N_3 ion gel were completely cross-linked, as shown in Figure 1b. As further evidence of the chemical cross-linking by UV irradiation, when 10 wt % SOS-N_3 ion gel was immersed in ethyl acetate, a good solvent for both EMI-TFSI and SOS-N_3 triblock copolymer, the uncross-linked physical ion gel quickly dissolved, whereas the UV-exposed SOS-N_3 ion gel could only swell in the solvent.

Morphological changes of the 10 wt % SOS-N_3 ion gel after UV exposure were investigated using small-angle X-ray scattering (SAXS). Figure 1c shows the SAXS profiles of the 10 wt % SOS-N_3 ion gels before and after UV cross-linking. Both scattering patterns are consistent with the Percus–Yevick hard sphere model that reflects a spherical form factor scattering in a liquid-like matrix.[40–42] The scattering patterns and structural model fits suggest that in 10 wt % SOS-N_3 ion gels a dense core formed by the PS-N_3 blocks (core radius ~6 nm) is surrounded by an outer shell of PEO blocks swollen by ionic liquid, and that this core structure is not affected by UV cross-linking. This provides evidence that the morphology of SOS-N_3 ion gels is not affected by photoinduced cross-linking, due to the confinement of the cross-linking reaction to the PS domains as shown in Figure 1d. Confinement of cross-linking in the PS-N_3 cores was also observed for thermally cross-linked SOS-N_3 ion gels.[34]

The electrical properties of 10 wt % SOS-N_3 ion gel films were measured using electrochemical impedance spectroscopy (EIS) before and after UV cross-linking. Metal-ion gel-metal (MIM) capacitors were fabricated by transferring a gold leaf top electrode onto a spin coated (or drop casted) ion gel film as depicted in the inset of Figure 2. The 10 wt % SOS-N_3 ion gel

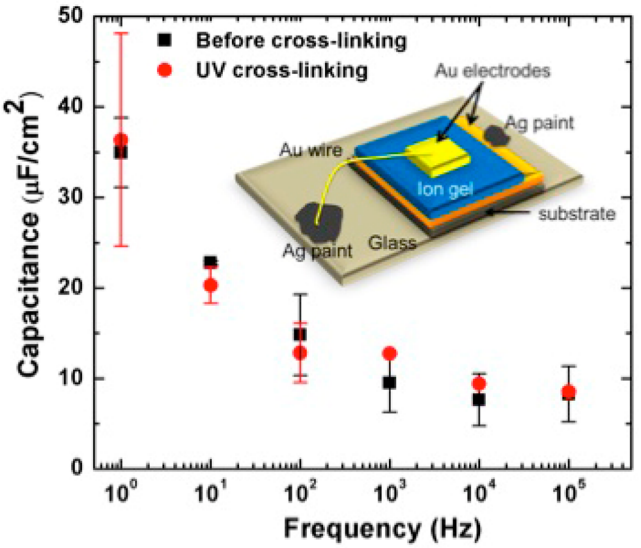

Figure 2. Frequency dependence of specific capacitance for 10 wt % SOS-N_3 ion gel films before chemical cross-linking and after UV irradiation for 90 min. The inset shows a schematic of the setup used for measuring impedance properties of Au/ion gel/Au capacitor.

films before and after UV cross-linking exhibited typical impedance behavior of electrolytes sandwiched by two solid electrodes (see the Supporting Information, Figure S1, for Nyquist plot and phase angle, Z', and Z'' versus frequency plots).[43] Figure 2 shows the calculated specific capacitance of 10 wt % SOS-N_3 ion gel films as a function of frequency before and after UV cross-linking. There is no significant difference in specific capacitance between uncross-linked and UV cross-linked ion gel films. The capacitance values in both ion gel films are greater than ~5 μF/cm^2 over the measured frequency range

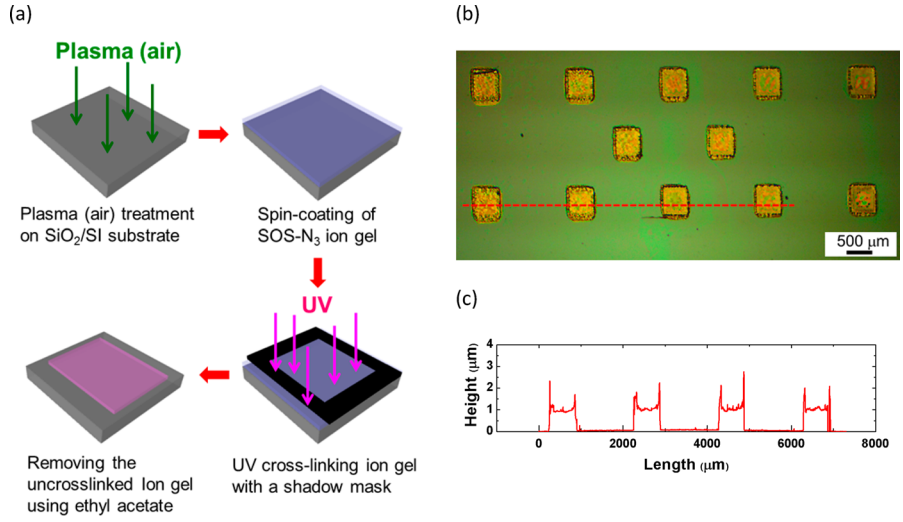

Figure 3. (a) Schematic procedures for the photopatterning of ion gel films using a shadow mask. (b) Optical micrograph of a photopatterned ion gel array on SiO_2/Si substrate. (c) Height profile of the photopatterned ion gels along the red dashed line in b. The thickness of the patterned ion gel is ~1.0 μm.

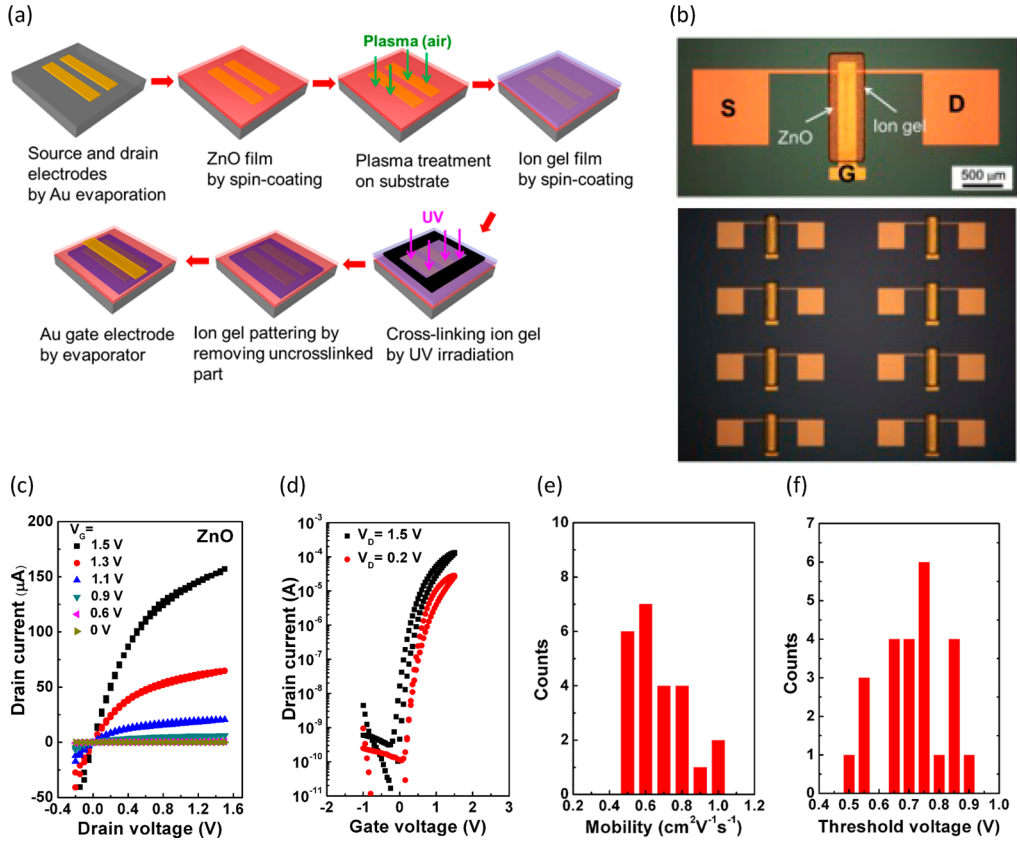

Figure 4. (a) Schematic procedures for fabricating ZnO thin film transistor using conventional shadow mask patterning processes. (b) Optical images of a single photo patterned ion gel gated transistor and an array of TFTs on SiO_2 substrate. (c) Output and (d) transfer characteristics of ZnO TFTs (n-type transistor) with photopatterned ion gel. Statistical summary of the device characteristics for 24 TFTs with photo patterned ion gel insulators: (e) saturation electron mobility and (f) threshold voltage. The channel length and width are 10 and 1000 μm, respectively. The gate voltage was swept at a rate of 50 mV/s.

(1−100 kHz) and increase with decreasing frequency. The large capacitance of 10 wt % SOS-N_3 ion gels in the range of 5−35 μF/cm^2 is due to the formation of the electric double layers at the electrode/ion gel interfaces. It should be noted that a frequency dependent capacitance at low frequencies can be attributed to capacitance dispersion that is related to the surface roughness of the solid electrodes.[44,45] It is expected that the 500 nm-thick Au leaf manually transferred on ion gels as a top electrode provides a somewhat inhomogeneous electrode surface. The measured ionic conductivity of the UV cross-linked 10 wt % SOS-N_3 ion gel film is ~2 mS/cm, which is also not affected by chemical cross-linking. This suggests that the

cores cross-linked by UV irradiation have no influence on ion transport properties in ion gels, which is consistent with previous observations in thermally cross-linked ion gels.[34]

Chemical cross-linking by UV irradiation allows a physical gel to be deposited on substrates and selectively cross-linked on the desired area. Figure 3a illustrates the procedure for photopatterning the chemically cross-linkable SOS-N_3 ion gels. The SiO_2/Si substrate was exposed to air plasma for 2 min to create hydroxyl groups on the surface. The 10 wt % SOS-N_3 ion gel films were deposited on the treated substrate by spin-coating. We speculate that the generated hydroxyl groups on the surface form hydrogen bonds with the PEO chains of SOS-N_3 ion gels, which improves the adhesion between the spin-coated ion gel film/substrate interfaces. After removing the residual solvent, a patterned metal shadow mask was placed on the ion gel films. The UV cross-linking reaction was conducted using a UV lamp (254 nm, 1.29 mW/cm^2) in a glovebox for 40−60 min. The part of the ion gel exposed to UV irradiation was chemically cross-linked whereas the unexposed part remained only physically cross-linked. After placing the sample in ethyl acetate (or chloroform) for 10 s, the uncross-linked ion gel was dissolved and removed, leaving only the chemically cross-linked patterned areas. Figure 3b displays an array of square-shaped ion gel patches created on the substrate by this process. The side of each square is ∼500 μm. Figure 3c displays a height profile of the square patches measured by a surface profiler. The measured thickness is ∼1 μm. Previously reported photo patternable cross-linked ion gels involved a photo-induced sol-to-gel transition,[24,31] whereas our approach involves a photoinduced physical-to-chemical-gel transition. This strategy allows a physical ion gel to be deposited onto the semiconductor layer prior to chemical cross-linking. Therefore, the thickness of the patterned ion gel was tuned easily by changing the solution concentration or spin speed, which is an important factor for better frequency response (i.e., less capacitance dispersion because of a smaller *RC* time constant for polarization), because the resistance of the ion gel is directly proportional to gel thickness.[43]

Photopatterning of the ion gels was employed in the fabrication of electrolyte gated thin film transistors as shown in the schematic procedures in Figure 4a. Photolithographically patterned Au source−drain (S−D) electrodes were used as bottom contacts. The devices have channel lengths and widths of 10 and 1000 μm, respectively. A 15 nm thick ZnO thin film was prepared by spin coating from a ZnO precursor solution and annealing at 300 °C. This produces a high performance n-type ZnO active layer by transforming the $Zn(OH)_2$ component into ZnO.[30,36] Next, ion gel was spin-coated onto the ZnO and then was photopatterned using the processes described above. Finally, a gold gate electrode was thermally evaporated on top of the patterned ion gel layer through another shadow mask. Figure 4b shows optical images of a single ion gel gated TFT and of an array of TFTs on SiO_2 substrate. The size and placement of the ion gel patches were simply controlled through the shadow masking procedures described above.

Figure 4c displays the output characteristics (drain current versus drain voltage) of a photo patterned ion gel gated ZnO transistor at six different gate voltages (V_G). The output curves exhibited good linearity at low drain voltages, and saturation at high voltages, as expected. This behavior indicates that the channel current increases with increasing V_G. Figure 4d shows the transfer curve (drain current versus gate voltage) of a ZnO TFT. The transfer characteristic was measured by sweeping V_G from −1 to 1.5 V and back to −1 V at a sweep rate of 50 mV/s. The transistor exhibited an ON/OFF current ratio of ∼1 × 10^5 and a small current hysteresis between forward and reverse V_G traces. The operation of n-type ZnO transistors at low voltages can be attributed to the high capacitance of the EDLs under positive gate bias, where mobile electrons are induced in the semiconductor by the accumulated cations at the ion gel/ZnO interface. The measured capacitance is ∼6 μF/cm^2, which is obtained from displacement current measurements on TFTs (see the Supporting Information Figure S2).[46] The electron mobility in the saturation regime was calculated from the following equation

$$I_D = \frac{W}{2L} C\mu (V_G - V_{th})^2 \quad (1)$$

where C is the capacitance of the gate insulator, W is the channel width, L is the channel length, V_{th} is the threshold voltage, and μ is the field-effect mobility. The V_{th} obtained from plot of $I_D^{1/2}$ versus V_G is 0.64 V and the saturation charge carrier mobility is 0.8 cm^2/(V s).

Panels e and f in Figure 4 summarize the transistor properties of 24 pattered ion gel gated TFTs in different batches. The average electron mobility and threshold voltages are 0.66 ± 0.14 cm^2/ (V s) and 0.71 ± 0.11 V, respectively. The devices also exhibited an average ON/OFF current ratio of 2.9 ± 0.9 × 10^5. There were no significant differences in mobility, threshold voltage, and ON/OFF current ratio between individual transistors. This high reproducibility implies that photo-patterning of the ion gel is a reliable process option in TFT fabrication.

We also constructed p-type organic TFTs through a combination of photopatterning of an ion gel dielectric and aerosol jet printing[19,30] of the polymer semiconductor regioregular poly(3-hexylthiophene) (P3HT) (see the Supporting Information, Figure S3). Both the transfer and output characteristics of the devices exhibited good linear and saturation behavior at low and high drain voltages, respectively. The average hole mobility in the saturation regime was 1.4 ± 0.4 cm^2/(V s) and the devices showed an ON/OFF current ratio of ∼1 × 10^5. This indicates that the performance of an organic semiconductor thin film is not affected by photo-pattering processes in the ion gel.

Importantly, it also turns out that we are able to thermally evaporate metal electrodes on the photopatterned ion gel, which is a substantial improvement in overall process flexibility. Because the surfaces of previously reported physically cross-linked ion gels were soft (modulus ≤1 × 10^4 Pa), there were limitations on the subsequent deposition of materials on the ion gels, either from solution or from the vapor phase. That is, thermal evaporation of metal, for example, on our previously reported ion gels yielded shorts, presumably because the metal simply penetrated the soft gel during deposition. The photopatterned ion gels, on the other hand, appear to be robust to the deposition of silver and gold, the two metals we have tried so far. We hypothesize that a small amount of ionic liquid leaching from the chemically cross-linked SOS-N_3 ion gel surface during the dissolution step of the patterning process leads to the creation of a robust "rubbery skin" on the patterned ion gels that serves as a kind of barrier to metal diffusion during deposition. The precise microstructural features of the photopatterned gels require further investigation. Nevertheless, the photopatterning and subsequent solvent dissolution of the

un-cross-linked regions of the gel have resulted in gels that can withstand a subsequent metal deposition step.

We have also determined that the measured ionic conductivity (~0.2 mS/cm) of the patterned SOS-N_3 ion gel films in MIM capacitors was reduced slightly, although we are still able to obtain large capacitances of ~1 μF/cm^2 at 100 kHz (see the Supporting Information, Figure S4). A reduction in electrical performance should be weighed against the gains in processability described above. The chemically cross-linked SOS-N_3 ion gel is also thermally stable under annealing conditions, as commonly required for sintering of metal nanoparticle inks.

CONCLUSIONS

We have demonstrated a photopatternable ion gel material that can be incorporated easily as a high capacitance gate insulator layer in TFTs. The ion gel is based on a triblock copolymer with azide groups in the end blocks that can be cross-linked by UV irradiation. Impedance spectroscopy and small-angle X-ray scattering confirmed that ion transport and the microstructure of the ion gels were not affected by UV cross-linking. The UV cross-linking photochemistry provides a convenient strategy to pattern layers of the ion gel by UV irradiation through a shadow mask. Arrays of thin film transistors with photopatterned ion gel gate insulator exhibited very uniform electrical characteristics. In particular, both P3HT and ZnO TFTs displayed simultaneous low voltage operation (<2 V supply) and high device performance (hole mobility of ~1.4 cm^2/(V s), electron mobility of ~0.7 cm^2/(V s), and ON/OFF current ratio of ~1 × 10^5) enabled by the high capacitance gate insulator. Furthermore, the UV exposure and postprocessing of the ion gel allow subsequent deposition of metals on top of the ion gel, without the formation of gate-to-channel shorts. We anticipate that the use of photopatterning processes will lead to new opportunities to conveniently incorporate ion gels into TFTs using conventional lithographic techniques.

ASSOCIATED CONTENT

Supporting Information

Impedance results for ion gel film after UV cross-linking, displacement current measurement, device characteristics of a P3HT TFT, and impedance results for photopatterned ion gel thin film. This material is available free of charge via the Internet at http://pubs.acs.org.

AUTHOR INFORMATION

Corresponding Authors

*E-mail: frisbie@umn.edu.
*E-mail: lodge@umn.edu.

Notes

The authors declare no competing financial interest.

ACKNOWLEDGMENTS

This work was supported by the Air Force Office of Scientific Research (FA9550-12-1-0067). The authors thank Chang-Hyun Kim for helpful discussions in designing shadow masks and Scott White for experimental assistance.

REFERENCES

(1) Facchetti, A. Gels Excel. *Nat. Mater.* **2008**, *7*, 839−840.
(2) Berggren, M.; Richter-Dahlfors, A. Organic Bioelectronics. *Adv. Mater.* **2007**, *19*, 3201−3213.
(3) Andersson, P.; Forchheimer, R.; Tehrani, P.; Berggren, M. Printable All-Organic Electrochromic Active-Matrix Displays. *Adv. Funct. Mater.* **2007**, *17*, 3074−3082.
(4) Cho, J. H.; Lee, J.; Xia, Y.; Kim, B.; He, Y.; Renn, M. J.; Lodge, T. P.; Frisbie, C. D. Printable Ion-Gel Gate Dielectrics for Low-Voltage Polymer Thin-Film Transistors on Plastic. *Nat. Mater.* **2008**, *7*, 900−906.
(5) Andersson, P.; Nilsson, D.; Svensson, P.-O.; Chen, M.; Malmström, A.; Remonen, T.; Kugler, T.; Berggren, M. Active Matrix Displays Based on All-Organic Electrochemical Smart Pixels Printed on Paper. *Adv. Mater.* **2002**, *14*, 1460−1464.
(6) Yamada, Y.; Ueno, K.; Fukumura, T.; Yuan, H. T.; Shimotani, H.; Iwasa, Y.; Gu, L.; Tsukimoto, S.; Ikuhara, Y.; Kawasaki, M. Electronically Induced Ferromagnetism at Room Temperature in Cobalt-Doped Titanium Dioxide. *Science* **2011**, *332*, 1065−1067.
(7) Ueno, K.; Nakamura, S.; Shimotani, H.; Ohtomo, A.; Kimura, N.; Nojima, T.; Aoki, H.; Iwasa, Y.; Kawasaki, M. Electric-field-induced Superconductivity in an Insulator. *Nat. Mater.* **2008**, *7*, 855−858.
(8) Herlogsson, L.; Noh, Y.-Y.; Zhao, N.; Crispin, X.; Sirringhaus, H.; Berggren, M. Downscaling of Organic Field-Effect Transistors with a Polyelectrolyte Gate Insulator. *Adv. Mater.* **2008**, *20*, 4708−4713.
(9) Hamedi, M.; Herlogsson, L.; Crispin, X.; Marcilla, R.; Berggren, M.; Inganäs, O. Fiber-Embedded Electrolyte-Gated Field-Effect Transistors for e-Textiles. *Adv. Mater.* **2009**, *21*, 573−577.
(10) Herlogsson, L.; Crispin, X.; Tierney, S.; Berggren, M. Polyelectrolyte-Gated Organic Complementary Circuits Operating at Low Power and Voltage. *Adv. Mater.* **2011**, *23*, 4684−4689.
(11) Fabiano, S.; Crispin, X.; Berggren, M. Ferroelectric Polarization Induces Electric Double Layer Bistability in Electrolyte-Gated Field-Effect Transistors. *ACS Appl. Mater. Interfaces* **2014**, *6*, 438−442.
(12) Thiemann, S.; Gruber, M.; Lokteva, I.; Hirschmann, J.; Halik, M.; Zaumseil, J. High-Mobility ZnO Nanorod Field-Effect Transistors by Self-Alignment and Electrolyte-Gating. *ACS Appl. Mater. Interfaces* **2013**, *5*, 1656−1662.
(13) Dhoot, A. S.; Israel, C.; Moya, X.; Mathur, N. D.; Friend, R. H. Large Electric Field Effect in Electrolyte-Gated Manganites. *Phys. Rev. Lett.* **2009**, *102*, 136402.
(14) Park, Y. D.; Kang, B.; Lim, H. S.; Cho, K.; Kang, M. S.; Cho, J. H. Polyelectrolyte Interlayer for Ultra-Sensitive Organic Transistor Humidity Sensors. *ACS Appl. Mater. Interfaces* **2013**, *5*, 8591−8596.
(15) Ha, M.; Xia, Y.; Green, A. A.; Zhang, W.; Renn, M. J.; Kim, C. H.; Hersam, M. C.; Frisbie, C. D. Printed, Sub-3V Digital Circuits on Plastic from Aqueous Carbon Nanotube Inks. *ACS Nano* **2010**, *4*, 4388−4395.
(16) Kim, S. H.; Hong, K.; Xie, W.; Lee, K. H.; Zhang, S.; Lodge, T. P.; Frisbie, C. D. Electrolyte-Gated Transistors for Organic and Printed Electronics. *Adv. Mater.* **2013**, *25*, 1822−1846.
(17) Xie, W.; Frisbie, C. D. Electrolyte Gated Single-Crystal Organic Transistors to Examine Transport in the High Carrier Density Regime. *MRS Bull.* **2013**, *38*, 43−50.
(18) Lee, J.; Panzer, M. J.; He, Y.; Lodge, T. P.; Frisbie, C. D. Ion Gel Gated Polymer Thin-Film Transistors. *J. Am. Chem. Soc.* **2007**, *129*, 4532−4533.
(19) Kim, S. H.; Hong, K.; Lee, K. H.; Frisbie, C. D. Performance and Stability of Aerosol-Jet-Printed Electrolyte-Gated Transistors Based on Poly(3-hexylthiophene). *ACS Appl. Mater. Interfaces* **2013**, *5*, 6580−6585.
(20) Lee, K. H.; Kang, M. S.; Zhang, S.; Gu, Y.; Lodge, T. P.; Frisbie, C. D. Cut and Stick" Rubbery Ion Gels as High Capacitance Gate Dielectrics. *Adv. Mater.* **2012**, *24*, 4457−4462.
(21) Lee, K. H.; Zhang, S.; Gu, Y.; Lodge, T. P.; Frisbie, C. D. Transfer Printing of Thermoreversible Ion Gels for Flexible Electronics. *ACS Appl. Mater. Interfaces* **2013**, *5*, 9522−9527.
(22) Cho, J. H.; Lee, J.; He, Y.; Kim, B.; Lodge, T. P.; Frisbie, C. D. High-Capacitance Ion Gel Gate Dielectrics with Faster Polarization Response Times for Organic Thin Film Transistors. *Adv. Mater.* **2008**, *20*, 686−690.

(23) Yomogida, Y.; Pu, J.; Shimotani, H.; Ono, S.; Hotta, S.; Iwasa, Y.; Takenobu, T. Ambipolar Organic Single-Crystal Transistors Based on Ion Gels. *Adv. Mater.* **2012**, *24*, 4392−4397.
(24) Lee, S. W.; Lee, H. J.; Choi, J. H.; Koh, W. G.; Myoung, J. M.; Hur, J. H.; Park, J. J.; Cho, J. H.; Jeong, U. Periodic Array of Polyelectrolyte-Gated Organic Transistors from Electrospun Poly(3-hexylthiophene) Nanofibers. *Nano Lett.* **2010**, *10*, 347−351.
(25) Bhat, S. N.; Pietro, R. D.; Sirringhaus, H. Electroluminescence in Ion-Gel Gated Conjugated Polymer Field-Effect Transistors. *Chem. Mater.* **2012**, *24*, 4060−4067.
(26) Kim, B. J.; Lee, S.-K.; Kang, M. S.; Ahn, J.-H.; Cho, J. H. Coplanar-Gate Transparent Graphene Transistors and Inverters on Plastic. *ACS Nano* **2012**, *6*, 8646−8651.
(27) Lee, S.-K.; Kim, B. J.; Jang, H.; Yoon, S. C.; Lee, C.; Hong, B. H.; Rogers, J. A.; Cho, J. H.; Ahn, J.-H. Stretchable Graphene Transistors with Printed Dielectrics and Gate Electrodes. *Nano Lett.* **2011**, *11*, 4642−4646.
(28) Pu, J.; Yomogida, Y.; Liu, K.-K.; Li, L.-J.; Iwasa, Y.; Takenobu, T. Highly Flexible MoS_2 Thin-Film Transistors with Ion Gel Dielectrics. *Nano Lett.* **2012**, *12*, 4013−4017.
(29) Thiemann, S.; Sachnov, S. J.; Pettersson, F.; Bollström, R.; Österbacka, R.; Wasserscheid, P.; Zaumseil, J. Cellulose-Based Ionogels for Paper Electronics. *Adv. Funct. Mater.* **2014**, *24*, 625−634.
(30) Hong, K.; Kim, S. H.; Lee, K. H.; Frisbie, C. D. Printed, sub-2V ZnO Electrolyte Gated Transistors and Inverters on Plastic. *Adv. Mater.* **2013**, *25*, 3413−3418.
(31) Choi, J.-H.; Lee, S. W.; Kar, J. P.; Das, S. N.; Jeon, J.; Moon, K.-J.; Lee, T. I.; Jeong, U.; Myoung, J.-M. Random Network Transistor Arrays of Embedded ZnO Nanorods in Ion-Gel Gate Dielectrics. *J. Mater. Chem.* **2010**, *20*, 7393−7397.
(32) Kang, M. S.; Lee, J.; Norris, D. J.; Frisbie, C. D. High Carrier Densities Achieved at Low Voltages in Ambipolar PbSe Nanocrystal Thin-Film Transistors. *Nano Lett.* **2009**, *9*, 3848−3852.
(33) Lodge, T. P. A Unique Platform for Materials Design. *Science* **2008**, *321*, 50−51.
(34) Gu, Y.; Zhang, S.; Martinetti, L.; Lee, K. H.; McIntosh, L. D.; Frisbie, C. D.; Lodge, T. P. High Toughness, High Conductivity Ion Gels by Sequential Triblock Copolymer Self-Assembly and Chemical Cross-Linking. *J. Am. Chem. Soc.* **2013**, *135*, 9652−9655.
(35) Susan, M. A. B. H.; Kaneko, T.; Noda, A.; Watanabe, M. Ion Gels Prepared by in Situ Radical Polymerization of Vinyl Monomers in an Ionic Liquid and Their Characterization as Polymer Electrolytes. *J. Am. Chem. Soc.* **2005**, *127*, 4976−4983.
(36) Park, S. Y.; Kim, B. J.; Kim, K.; Kang, M. S.; Lim, K.-H.; Lee, T. L.; Myoung, J. M.; Baik, H. K.; Cho, J. H.; Kim, Y. S. Low-Temperature, Solution-Processed and Alkali Metal Doped ZnO for High-Performance Thin-Film Transistors. *Adv. Mater.* **2012**, *24*, 834−838.
(37) Bang, J.; Bae, J.; Löwenhielm, P.; Spiessberger, C.; Given-Beck, S. A.; Russell, T. P.; Hawker, C. J. Facile Routes to Patterned Surface Neutralization Layers for Block Copolymer Lithography. *Adv. Mater.* **2007**, *19*, 4552−4557.
(38) Yoo, M.; Kim, S.; Lim, J.; Kramer, E. J.; Hawker, C. J.; Kim, B. J.; Bang, J. Facile Synthesis of Thermally Stable Core-Shell Gold Nanoparticles via Photo-Cross-Linkable Polymeric Ligands. *Macromolecules* **2010**, *43*, 3570−3575.
(39) Lee, S.; Lee, B.; Kim, B. J.; Park, J.; Yoo, M.; Bae, W. K.; Char, K.; Hawker, C. J.; Bang, J.; Cho, J. Free-Standing Nanocomposite Multilayers with Various Length Scales, Adjustable Internal Structures, and Functionalities. *J. Am. Chem. Soc.* **2009**, *131*, 2579−2587.
(40) Percus, J. K.; Yevick, G. J. Analysis of Classical Statistical Mechanics by Means of Collective Coordinates. *Phys. Rev.* **1958**, *110*, 1−13.
(41) Kinning, D. J.; Thomas, E. L. Hard-Sphere Interactions between Spherical Domains in Diblock Copolymers. *Macromolecules* **1984**, *17*, 1712−1718.
(42) Kinning, D. J.; Thomas, E. L.; Fetters, L. J. Morphological Studies of Micelle Formation in Block Copolymer/homopolymer blends. *J. Chem. Phys.* **1989**, *90*, 5806−5825.
(43) Lee, K. H.; Zhang, S.; Lodge, T. P.; Frisbie, C. D. Electrical Impedance of Spin-Coatable Ion Gel Films. *J. Phys. Chem. B* **2011**, *115*, 3315−3321.
(44) Brug, G. J.; Van den Eeden, A. L. G.; Sluyters-Rehbach, M.; Sluyters, J. H. The Analysis of Electrode Impedances Complicated by the Presence of a Constant Phase Element. *J. Electroanal. Chem.* **1984**, *176*, 275−295.
(45) Pajkossy, T. Impedance of Rough Capacitive Electrodes. *J. Electroanal. Chem.* **1994**, *364*, 111−125.
(46) Xie, W.; Frisbie, C. D. Organic Electrical Double Layer Transistors Based on Rubrene Single Crystals: Examining Transport at High Surface Charge Densities above 10^{13} cm^{-2}. *J. Phys. Chem. C* **2011**, *115*, 14360−14368.